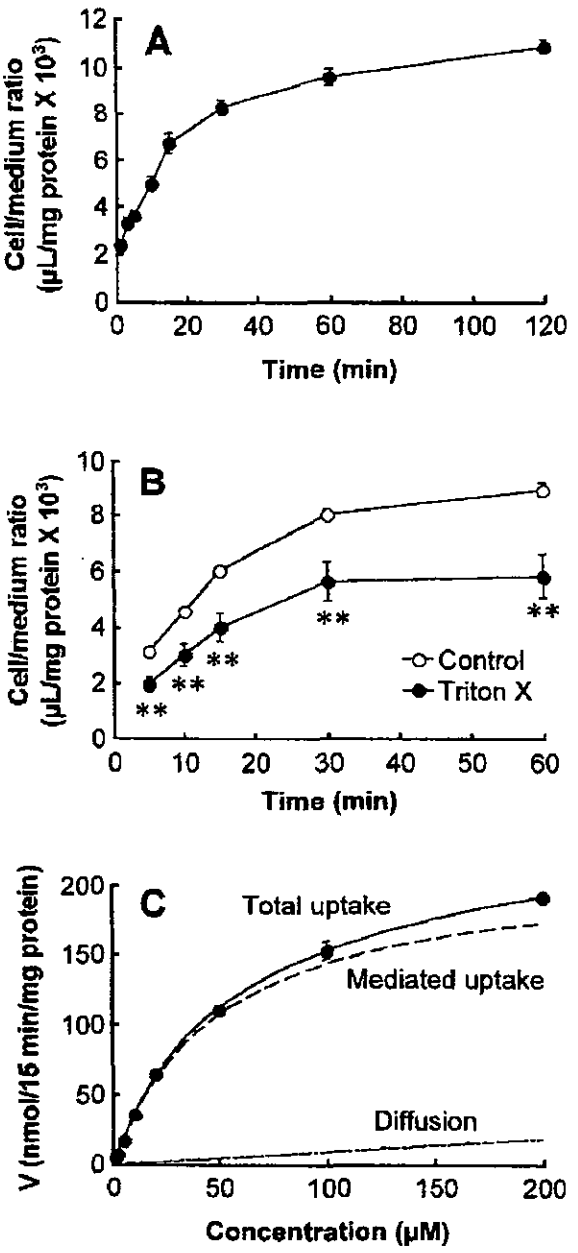

Fig. 2. Characteristics of quinacrine uptake by MBEC4 cells. Panel (A), time course of quinacrine (1 μM) uptake by MBEC4 cells. Panel (B), changes in the quinacrine (1 μM) uptake by MBEC4 cells exposed to 0.015% Triton X for 10 min before the uptake experiment. Panel (C), concentration-dependence of quinacrine uptake by MBEC4 cells. Initial uptake rates at various concentrations of quinacrine (1–200 μM) were measured at 37°C for 15 min. Curves for total, mediated, and diffusive uptake were drawn using the parameters obtained from nonlinear regression analysis (MULTI). Each point represents the mean ± SEM. ($n = 4$–20).** $P < 0.01$: significant difference from the control.

Table I. Effects of Various Compounds and Sodium-Replacement on Uptake of Quinacrine (1 μM) by MBEC4 Cells

Condition	Concentration	Cell/medium ratio (% of control)
NaN_3	10 mM	$67.2 \pm 3.03^{a,**}$
DNP	1 mM	$70.2 \pm 1.79^{a,**}$
4°C		$18.6 \pm 2.22^{a,**}$
FCCP	10 μM	$77.4 \pm 2.49^{a,**}$
Valinomycin	10 μM	97.2 ± 4.22^{a}
Amiloride	1 mM	97.4 ± 3.16^{a}
Tetraethylammonium	1 mM	$88.0 \pm 2.95^{b,**}$
	5 mM	$84.3 \pm 2.93^{b,**}$
	10 mM	$75.4 \pm 4.15^{b,**}$
Cimetidine	1 mM	$81.3 \pm 5.56^{c,**}$
	5 mM	$57.8 \pm 1.70^{c,**}$
	10 mM	$36.8 \pm 1.61^{c,**}$
Na^+ replacement with N-methylglucamine		104 ± 2.87^{d}

[a]MBEC4 cells were preincubated with NaN_3, DNP, FCCP, valinomycin, or amiloride for 10 min. Control values were $4.9 \pm 0.42 \times 10^3$ μL/mg protein. [b,c]Quinacrine uptake was measured by incubating MBEC4 cells with TEA or cimetidine. Control values were 4.1 ± 0.19 and $5.2 \pm 0.19 \times 10^3$ μL/mg protein, respectively.
[d]For investigation of the sodium dependency, quinacrine uptake was measured where Na^+ in the uptake buffer was replaced by N-methylglucamine. Control values were $3.6 \pm 0.22 \times 10^3$ μL/mg protein. Quinacrine uptake was measured at 37°C for 15 min. Values are expressed as % of control. Values are shown as means ± SEM ($n = 4$–20).
**$P < 0.01$; significant difference from the control.

(Fig. 3(B)). These findings demonstrated that quinacrine uptake by MBEC4 cells was pH-dependent. Pretreatment with 10 mM of NaN_3 inhibited quinacrine uptake at each pH used (Table II). Quinacrine uptake was not affected by 1 mM of amiloride (Table I). Therefore, quinacrine uptake was found to be unaffected by Na^+/H^+

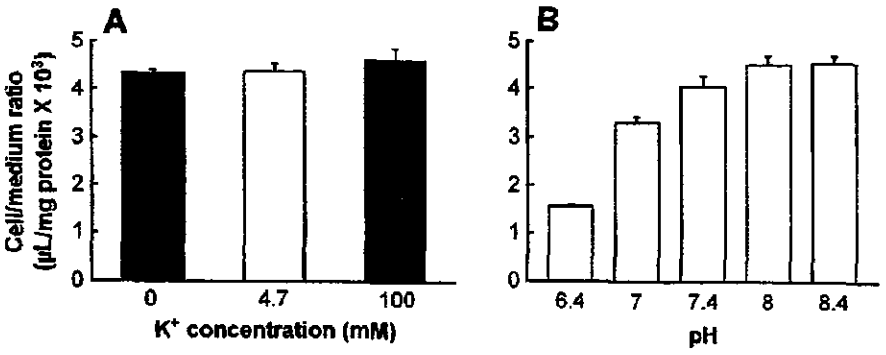

Fig. 3. Effects of the membrane potential (A) and pH (B) on the uptake of quinacrine (1 μM) by MBEC4 cells. Panel (A), effects of various concentrations of external potassium on quinacrine uptake: 0 mM (hyperpolarized), 4.7 mM (control), or 100 mM (depolarized). Panel (B), effects of various pH of the medium on quinacrine uptake. Quinacrine uptake was measured at 37°C for 15 min. Values are expressed as the cell-to-medium ratios. Values are shown as means ± SEM. ($n = 12$).

Table II. Effect of ATP Depletion on the Uptake of Quinacrine (1 μM) by MBEC4 Cells

pH	Cell/medium ratio (μL/mg protein $\times 10^3$)	
	Normal	ATP-depletion
6.4	1.61 ± 0.02	1.36 ± 0.03**
7.0	3.53 ± 0.14	3.28 ± 0.10
7.4	3.95 ± 0.32	3.20 ± 0.33*
8.0	4.71 ± 0.35	3.87 ± 0.30
8.4	4.77 ± 0.19	3.82 ± 0.22*

MBEC4 cells were preincubated with 10 mM NaN_3 for 10 min (ATP depletion). Quinacrine uptake was measured at 37°C for 15 min. Values are shown as means ± SEM ($n = 3$–8).
*$P < 0.05$, **$P < 0.01$; significant difference from the control.

exchange. The effects of organic cations and P-gp inhibitors on quinacrine uptake were investigated. The organic cations including TEA (1-10 mM) and cimetidine (1–10 mM) significantly reduced quinacrine uptake by 12–25% and 19–65%, respectively (Table I). In the presence of cyclosporine (10 μM) or verapamil (20 μM), quinacrine uptake under the steady-state significantly increased by about 10% (Fig. 4).

To provide molecular evidence for the expression of OCTN1 in MBEC4 cells, RT-PCR was carried out (Fig. 5). With a primer pair specific for mouse OCTN1, RT-PCR with mRNA obtained from MBEC4 cells yielded a single product. The size of this product was the same as that expected from the primer positions in mouse OCTN1.

DISCUSSION

The BBB permeability coefficient of quinacrine, a candidate for the treatment of CJD, was much lower than that of Na-F, a BBB-impermeable marker, suggesting that

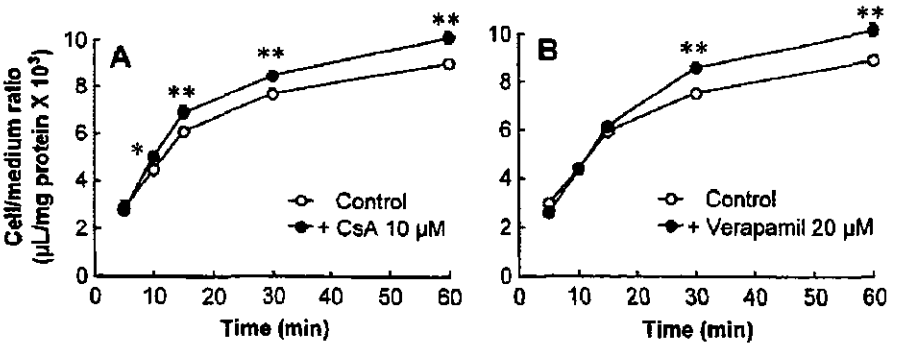

Fig. 4. Effects of 10 μM cyclosporine (A) and 20 μM verapamil (B) on uptake of quinacrine (1 μM) by MBEC4 cells. Quinacrine uptake was measured at 37°C in the absence and presence of cyclosporine or verapamil. Values are expressed as the cell-to-medium ratios. Values are shown as means ± SEM. ($n = 8$).

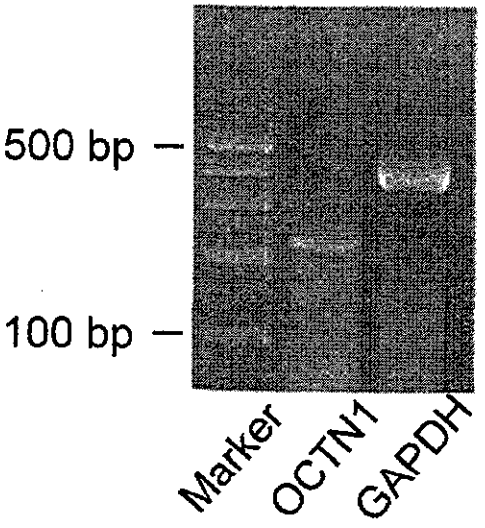

Fig. 5. Photograph showing OCTN1 expression in MBEC4 cells by RT-PCR. RNA samples from MBEC4 cells were used for RT-PCR with primer pairs specific for mouse OCTN1.

the permeability of quinacrine into the brain through the BBB is extremely low. To determine which machinery is involved in the low permeability of quinacrine across the BBB, we investigated the polarity of transcellular transport of quinacrine and the effects of P-gp inhibitors (cyclosporine and verapamil) on the BBB permeability of quinacrine. The basolateral-to-apical (brain-to-blood) transport of quinacrine across MBEC4 monolayer was greater than quinacrine transport in the opposite direction (Fig. 1(B)). Cyclosporine and verapamil increased the apical-to-basolateral (blood-to-brain) transport of quinacrine (Fig. 1(C)). Quinacrine uptake by MBEC4 cells under the steady-state was significantly increased by cyclosporine and verapamil (Fig. 4). These findings indicate the possible involvement of P-gp in the efflux transport of quinacrine. P-gp largely contributes to multidrug-resistance of the BBB in an ATP-dependent manner. This study provided controversial evidence that metabolic inhibitors or incubation at low temperature decreased quinacrine uptake (Table I). Quinacrine was actively and concentratively accumulated in MBEC4 cells. A large part of quinacrine is probably taken up via the saturable system, although quinacrine uptake was shown to have both saturable and nonsaturable pathways (Fig. 2(C)). Uptake of quinacrine by choroid plexus cells was organic cation-specific and energy-dependent (Miller *et al.*, 1999). In light of these findings, P-gp (an efflux system) and other influx transport system(s) are considered to mediate quinacrine transport into the brain.

We elucidated a role of the known organic cation transporters (OCT1, OCT2, OCT3, OCTN1, and OCTN2), and the specificity or driving force of those transporters in mediating quinacrine uptake by MBEC4 cells. Quinacrine uptake was significantly inhibited by various organic cations including TEA and cimetidine, which are known to be a substrate and an inhibitor of the organic cation transporters, respectively. Quinacrine uptake was insensitive to changes in the membrane potential (Fig. 3(A)) and strongly inhibited by lowering the external pH (Fig. 3(B)). These characteristics are distinct from those of the OCT1, OCT2, and OCT3, all of which

are dependent on the membrane potential (Gorboulev *et al.*, 1997; Grundemann *et al.*, 1994; Kekuda *et al.*, 1998). Considering quinacrine is an organic base, the pH-related decrease in quinacrine uptake may have resulted from an increase in the concentration of ionized quinacrine according to the pH partition theory. However, our data showing that quinacrine uptake by MBEC4 cells at each pH was inhibited by NaN_3 (Table II) suggest that a pH-sensitive transport system is involved in quinacrine uptake. Transport of quinacrine increased by elevating the outward H^+ gradient across the membrane. This finding indicates that quinacrine may be transported through MBEC4 cells by an H^+/quinacrine antiport. The activity of H^+/organic cation antiporter is regulated by pH or H^+ gradient as the driving force (Maegawa *et al.*, 1988). The H^+ gradient is formed by Na^+/H^+ exchange in the vicinity of the apical membrane of brain endothelial cells (Ennis *et al.*, 1996). The Na^+/H^+ exchange is, however, unlikely to participate in quinacrine uptake by MBEC4 cells, since Na^+-depletion and amiloride failed to reduce quinacrine uptake (Table I). OCTN1 is Na^+-independent organic cation transporter (Wu *et al.*, 2000). OCTN2 mediates uptake of L-carnitine and several organic cations in an Na^+-coupled and Na^+-independent manner, respectively (Wu *et al.*, 1999). OCTN1 is a pH-dependent organic cation transporter presumably energized by a proton antiport mechanism (Yabuuchi *et al.*, 1999). The characteristics of quinacrine transport obtained in this study are similar to those of OCTN1. Mouse OCTN1 is distributed in the brain, heart, and liver, and strongly expressed in the kidney (Tamai *et al.*, 2000). RT-PCR analysis of MBEC4 cells demonstrated the expression of OCTN1 (Fig. 5). Therefore, OCTN1 is suggested to be a potential transporter mediating quinacrine uptake by MBEC4 cells.

The BBB permeability of quinacrine was extremely low, although quinacrine was rapidly transported into the brain endothelial cells by the apical pH-dependent transport system. A weak organic base binds to a variety of polyanions including RNA, DNA, and ATP, and accumulates in the acidic intracellular compartments (Miller *et al.*, 1999). Quinacrine is distributed in the nucleus and vesicular compartment in the cytoplasm of choroid plexus cells (Miller *et al.*, 1999). In the brain endothelial cells, a large part of quinacrine was shown to be distributed and accumulated in the intracellular binding compartment (Fig. 2(B)). The resulting small part of quinacrine in the intracellular nonbinding compartment appears to contribute to the BBB permeability. The P-gp-mediated active efflux at the apical side of the plasma membrane and the large storage capacity in the cytoplasm are considered to restrict the entry of quinacrine into the brain. The mechanism involved in quinacrine transport at the basolateral side remains obscure.

In conclusion, quinacrine transport at the BBB is mediated by the influx and efflux transport systems. The influx of quinacrine is mediated by a pH-dependent and Na^+- and membrane potential-independent system, an OCTN1-like transporter. The efflux of quinacrine evoked by P-gp at the BBB restricts the entry of quinacrine into the brain. This phenomenon may be interpreted as lowering the therapeutic efficacy of quinacrine for CJD. This study may have clinical implications; quinacrine concentrations in the brain increased by P-gp modulators including verapamil may enhance the therapeutic efficacy of quinacrine for CJD.

ACKNOWLEDGMENTS

This work was supported in part by a Grant-in-Aid for Scientific Research ((B)(2) 14370789) from the Ministry of Education, Culture, Sports, Science, and Technology (MEXT), Japan.

REFERENCES

Bradford, M. M. (1976). A rapid and sensitive method for the quantitation of microgram quantities of protein utilizing the principle of protein dye binding. *Anal. Biochem.* **72:**248–254.

Chan, B. S., Satriano, J. A., Pucci, M., and Schuster, V. L. (1998). Mechanism of prostaglandin E_2 transport across the plasma membrane of HeLa cells and Xenopus oocytes expressing the prostaglandin transporter "PGT". *J. Biol. Chem.* **273:**6689–6697.

Dehouck, M.-P., Jolliet-Riant, P., Brée, F., Fruchart, J.-C., Cecchelli, R., and Tillement, J.-P. (1992). Drug transfer across the blood–brain barrier: Correlation between in vitro and in vivo models. *J. Neurochem.* **58:**1790–1797.

Ennis, S. R., Ren, X., and Betz, A. L. (1996). Mechanisms of sodium transport at the blood-brain barrier studied with in situ perfusion of rat brain *J. Neruochem.* **66:**756–763.

Follette, P. (2003). Prion disease treatment's early promise unravels. *Science* **299:**191–192.

Friedrich, A., George, R. L., Bridges, C. C., Prasad, P. D., and Ganapathy, V. (2001). Transport of cholin and its relationship to the expression of organic cation transporters in a rat brain microvessel cell line (RBE4). *Biochim. Biophys. Acta* **1512:**299–307.

Friedrich, A., Prasad, P. D., Freyer, D., Ganapathy, V., and Brust, P. (2003). Molecular cloning and functional characterization of the OCTN2 transporter at the RBE4 cells, an in vitro model of the blood-brain barrier. *Brain Res.* **968:**69–79.

Gorboulev, V., Ulzheimer, J. C., Akhoundova, A., Ulzheimer-Teuber, I., Karbach, U., Quester, S., Baumann, C., Lang, F., Busch, A. E., and Koepsell, H. (1997). Cloning and characterization of two human polyspecific organic cation transporters. *DNA Cell Biol.* **16:**871–881.

Grundemann, D., Gorboulev, V., Gambaryan, M., Vehyhl, M., and Koepsell, H. (1994). Drug excretion mediated by a new prototype of polyspecific transporter. *Nature* **372:**549–552.

Kekuda, R., Prasad, P. D., Wu, X., Wang, H., Fei, Y. J., Leibach, F. H., and Ganapathy, V. (1998). Cloning and functional characterization of a potential-sensitive, polyspecific organic cation transporter (OCT3) most abundantly expressed in placenta. *J. Biol. Chem.* **273:**15971–15979.

Koepsell, H. (1998). Organic cation transporters in intestine, kidney, liver, and brain. *Annu. Rev. Physiol.* **60:**243–266.

Korth, C., May, B. C. H., Cohen, F. E., and Prusiner, S. B. (2001). Acridine and phenothiazine derivatives as pharmacotherapeutics for prion disease. *Proc. Natl. Acad. Sci. U.S.A.* **98:**9836–9841.

Maegawa, H., Kato, M., Inui, K., and Hori, R. (1988). pH sensitivity of H^+/organic cation antiport system in rat renal brush-border membranes. *J. Biol. Chem.* **263:**11150–11154.

Miller, D. S., Villalobos, A. R., and Pritchard, J. B. (1999). Organic cation transport in rat choroid plexus cells studied by fluorescence microscopy. *Am. J. Physiol.* **276:**C955–C968.

Okuda, N., Saito, H., Urakami, Y., Takano, M., and Inui, K. I. (1996). cDNA cloning and functional expression of a novel rat kidney organic cation transporter. *Biochem. Biophys. Res. Commun.* **224:**500–507.

Sawada, N., Takanaga, H., Matsuo, H., Naito, M., Tsuruo, T., and Sawada, Y. (1999). Choline uptake by mouse brain capillary endothelial cells in culture. *J. Pharm. Pharmacol.* **51:**847–852.

Sweet, D. H., and Pritchard, J. (1999). rOCT2 is a basolateral potential-driven carrier, not an organic cation/proton exchanger. *Am. J. Physiol.* **277:**F890–F898.

Tamai, I., Ohashi, R., Nezu, J., Sai, Y., Kobayashi, D., Oku, A., Shimane, M., and Tsuji, A. (2000). Molecular and functional characterization of organic cation/carnitine transporter family in mice. *J. Biol. Chem.* **275:**40064–40072.

Tamai, I., Yabuuchi, H., Nezu, J., Sai, Y., Oku, A., Shimane, M., and Tsuji, A. (1997). Cloning and characterization of a novel human pH-dependent organic cation transporter, OCTN1. *FEBS Lett.* **419:**107–111.

Tatsuta, T., Naito, M., Mikami, K., and Tsuruo, T. (1994). Enhanced expression by the brain matrix of P-glycoprotein in brain capillary endothelial cells. *Cell Growth Differ.* **5:**1145–1152.

Tatsuta, T., Naito, M., Oh-hara, T., Sugawara, I., and Tsuruo, T. (1992). Functional involvement of P-glycoprotein in blood–brain barrier. *J. Biol. Chem.* **267:**20383–20391.

Wu, X., George, R. L., Huang, W., Wang, H., Conway, S. J., Leibach, F. H., and Ganapathy, V. (2000). Structural and functional characteristics and tissue distribution pattern of rat OCTN1, an organic cation transporter, cloned from placenta. *Biochim. Biophys. Acta* **1466**:315–327.

Wu, X., Huang, W., Prasad, P. D., Seth, P., Rajan, D. P., Leibach, F. H., Chen, J., Conway, S. J., and Ganapathy, V. (1999). Functional characteristics and tissue distribution pattern of organic cation transporter 2 (OCTN2), an organic cation/carnitine transporter. *J. Pharmacol. Exp. Ther.* **290**:1482–1492.

Wu, X., Prasad, P. D., Leibach, F. H., and Ganapathy, V. (1998). cDNA sequence, transport function, and genomic organization of human OCTN2, a new member of the organic cation transporter family. *Biochem. Biophys. Res. Commun.* **246**:589–595.

Yabuuchi, H., Tamai, I., Nezu, J., Sakamoto, K., Oku, A., Shimane, M., Sai, Y., and Tsuji, A. (1999). Novel membrane transporter OCTN1 mediates multispecific, bidirectional, and pH-dependent transport of organic cations. *J. Pharmacol. Exp. Ther.* **289**:768–773.

Yamaoka, K., Tanigawara, Y., Nakagawa, T., and Uno, T. (1981). A pharmacokinetic analysis program (MULTI) for microcomputer. *J. Pharmacobiodyn.* **4**:879–885.

Original Research Article

Dementia and Geriatric Cognitive Disorders

Dement Geriatr Cogn Disord 2004;17:158–163
DOI: 10.1159/000076350

Accepted: June 30, 2003
Published online: January 20, 2004

Results of Quinacrine Administration to Patients with Creutzfeldt-Jakob Disease

Masashi Nakajima[a] Tatsuo Yamada[a] Tomohiko Kusuhara[a]
Hisako Furukawa[b] Mitsuo Takahashi[b] Atsushi Yamauchi[c]
Yasufumi Kataoka[c]

Departments of [a]Neurology, [b]Clinical Pharmacology and [c]Pharmaceutical Care and Health Sciences, Fukuoka University, Fukuoka, Japan

Key Words
Creutzfeldt-Jakob disease · Prion · Quinacrine

Abstract
Several chemicals inhibit the accumulation of abnormal prion proteins in vitro. We administered one, the antimalarial agent quinacrine, to three patients with sporadic Creutzfeldt-Jakob disease (CJD) and to one with iatrogenic CJD. Quinacrine at 300 mg/day was given enterally for 3 months. Within 2 weeks of administration, the arousal level of the patient with akinetic mutism improved. The other 3 patients, insensible before treatment, had integrative responses such as eye contact or voluntary movement in response to verbal and/or visual stimuli restored. Clinical improvement was transient, lasting 1–2 months during treatment. Quinacrine was well tolerated, except for liver dysfunction and yellowish pigmentation. Although its antiprion activity in the human brain has yet to be proved, these modest effects of quinacrine suggest the possibility of using chemical intervention against prion diseases.

Introduction

Creutzfeldt-Jakob disease (CJD), a prion-mediated disease in humans, is invariably fatal. Accumulation of the abnormal protease-resistant prion protein (PrP^{Sc}), formed posttranslationally from the normal endogenous protease-sensitive isoform (PrP^{c}), is a central event in CJD pathogenesis [1]. Recent outbreaks of a new variant of CJD in young people [2], and of iatrogenic CJD after cadaveric dura grafting [3], require that treatment be immediately available for dying humans. The antimalarial agent quinacrine has long been used to treat patients with malaria and giardiasis. Two recent reports found that quinacrine inhibits and eradicates PrP^{Sc} in scrapie-infected neuroblastoma cells [4, 5]. Korth et al. [5] found that of the acridine and phenothiazine derivatives they tested, quinacrine and chlorpromazine inhibited PrP^{Sc} accumulation, and they noted the importance of the aliphatic side chain on the middle ring moiety of tricyclic compounds. Quinacrine was 10 times more potent than chlorpromazine, its effective concentration for half-maximal inhibition (EC_{50}) of PrP^{Sc} formation being 300 n*M* [5] (400 n*M* in the report of Doh-Ura et al. [4]). After chronic oral administration of quinacrine to humans, its serum concentration exceeded 450 n*M* for a total dose of 4.5 g given over 6 days [6]. Quinacrine is also deposited in the brain [7], and the tissue to plasma concentration ratio

KARGER
Fax + 41 61 306 12 34
E-Mail karger@karger.ch
www.karger.com

1420–8008/04/0173–0158$21.00/0

Accessible online at:
www.karger.com/dem

Masashi Nakajima, MD
Department of Neurology, Tokyo Rosai Hospital
4-13-21 Ohmori-minami, Ohta-ku
Tokyo 143-0013 (Japan)
Tel. +81 3 3742 7301, Fax +81 3 3744 9310, E-Mail masashi@tokyoh.rofuku.go.jp

Table 1. *Clinical findings* before and after quinacrine treatment

Patient No./ age, years/ gender/Dx	Duration of illness	Before quinacrine administration		Feeding	After quinacrine administration		Duration of changes
		cognitive state	motility		cognitive state	motility	
1/46/M/ sCJD	11 months	akinetic mutism; roving eye movement; cortical blindness	eyes open to noxious stimuli; reflex myoclonus	NG tube	fixation of eyes	gaze oriented to the direction of a voice; decreased reflex myoclonus	from the 2nd to 5th week
2/58/M/ sCJD	2 months	alert; eye tracking for the object; startle response to visual, auditory and tactile stimuli; ignorance of object presented in the right visual field	withdrawal and purposeless movement; action myoclonus; paraplegia in flexion	NG tube	smiles at family members; eye tracking and startle response to an object presented in the right visual field	decreased action myoclonus	from the 6th day to the 6th week
3/61/F/ sCJD	2 months	alert; fearful, startle response; response to visual and auditory stimuli; right hemianopsia	withdrawal movement;	fed orally, or NG tube	increased eye contact with the examiner; laughter at visual and auditory stimuli	voluntary left arm movement and side-to-side head movement	from the 8th day to the 3rd week
4/58/F/ possibly iatrogenic CJD	6 years	alert; grimacing and moaning to noxious stimuli; listless to visual and auditory stimuli	palilalia; stereotyped limbs and orolingual movement; impossible to sit or stand up even with assistance	fed orally	apparent eye contact with people; laughter at visual and auditory stimuli; appropriate 'yes or no' to questions	able to sit up on a reclining chair	from the 2nd to 8th week

Dx = Diagnosis; NG = nasogastric.

is very high [8]. Its pharmacokinetics suggests that a concentration of quinacrine can be obtained in the human brain sufficient to inhibit abnormal prion accumulation, as shown in an in vitro experiment [4, 5].

Patients and Methods

Patients

Three patients with clinically probable sporadic CJD (sCJD; patients 1–3) and one with possible iatrogenic CJD which may have been transmitted by dura mater grafts (patient 4) were studied. Their ages, sex, duration of illness and status at the start of the study are given in table 1. These patients were admitted to Fukuoka University Hospital between October 2001 and February 2002. The three sCJD patients fulfilled the Masters', French and European criteria for probable CJD [9] and showed progressive dementia, myoclonus, visual or cerebellar signs, extrapyramidal signs, typical periodic sharp and slow wave complexes (PSWCs) on EEGs, and positive detection of CSF 14-3-3 proteins.

Patient 4 had undergone removal of a right cerebellopontine angle tumor and had had dura mater grafts in July 1991. She received a single brand of dura mater graft, LYODURA®, processed by B. Braun Melsungen AG before 1987, which brand was found to be responsible for a Japanese outbreak of iatrogenic CJD [3]. She developed progressive dementia in January 1996, became listless within 2 years, and was bedridden within 4 years of onset. Stereotyped repetitive limb movement (palikinesia) and a few patterns of simple sound repetition (palilalia) characterized her status. She moaned emotionally on manipulation of her limbs and had dysphasia, but swallowing was possible when fed. She had extrapyramidal rigidity and exaggerated tendon reflexes, but no ataxia, myoclonus, PSWCs or CSF 14-3-3 proteins. MRI showed diffuse cerebral atrophy. Nondegenerative dementias caused by anoxic brain damage or normal pressure hydrocephalus, and dementias of infectious, neoplastic, metabolic, nutritional or endocrine origin were excluded.

Methods

The four patients were administered 300 mg/day quinacrine enterally for 3 months. The study had been approved by our institution's ethics committee, and the patients' relatives had consented to the procedure. Quinacrine was given as 100 mg of powder in capsule form. It was administered orally 3 times a day after each meal, or through a nasogastric tube after being dissolved in water at 37°C. The patients' behavior and neurological examinations were videotaped every 2 weeks. Routine hematological and blood chemistry studies were done weekly, and EEGs were obtained every 2 weeks. Brain MRI that included diffusion-weighted (DW) images was done in the 4th and 12th weeks after treatment began. Quinacrine was withdrawn if major side effects such as convulsion, bone marrow suppression (white blood cell count <2,000/μl) or significant liver dysfunction (>5 times the normal upper limits for aspartate aminotransferase or alanine aminotransferase) occurred. In addition, if the patient's condition was complicated by infection, metabolic irregu-

larities or gastrointestinal problems, quinacrine was withdrawn and readministered only when the condition had returned to normal. No other medicines were given during the period of quinacrine administration. The plasma concentration of quinacrine in the patients' blood samples was measured by high-performance liquid chromatography.

Results

Quinacrine was well tolerated by all the patients. Yellowish skin pigmentation invariably appeared 10–14 days after treatment began. Transaminase values were elevated in 3 of the 4 patients, but never reached 5 times the normal upper limits. Patients 1 and 2 had quinacrine withdrawn temporarily because of aspiration pneumonia, urinary tract infection or diarrhea, but both finally completed the 3-month treatment course.

Clinical Course

A change in cognitive state appeared during the first 2 weeks of treatment (table 1). Patient 1's unfocused, occasionally roving eyes (fig. 1a) became fixed (fig. 1b) and sometimes were oriented to the side of auditory stimuli (fig. 1c). When stimulated, patients 2 and 3 showed mitigation of irritable mood and the return of smiles or laughter. Patient 3, who had been apathetic (fig. 1d), made apparent eye contact with people (fig. 1e), turned her head from side to side in response to the examiner's position, and had purposeful, voluntary movement of the left arm (fig. 1f). Patient 4 also made eye contact with people and nonpathological laughter in response to stimuli was restored. She also nodded or shook her head, apparently indicating 'yes' or 'no', in response to simple verbal questions such as those about pain or thirst.

These changes in mood or cognitive function were invariably transient, lasting 2–8 weeks during the period of quinacrine administration, after which cognitive function gradually decreased to baseline levels. Due to the associated conditions described previously, quinacrine was temporarily withdrawn from patient 1 in the 5th and patient 2 in the 6th week. Both patients' conditions deteriorated to akinetic mutism that remained even after quinacrine was restarted. After 3–8 weeks of treatment, cognitive function in patients 3 and 4 had regressed with no predisposing factors.

EEG and MRI Findings

Patient 2 showed changes in both EEG and MRI findings, which may be associated with the clinical changes that occurred. Typical PSWCs in the severely suppressed background before treatment (fig. 2a) had become irregular slow activities with less periodicity and no suppression by day 16 of treatment (fig. 2b). Before treatment, DW-MRI detected high signals bilaterally in the corpus striatum and insular and cingulate gyri, as well as in the temporal and parietal lobes. The signal intensities in the temporal and parietal lobe lesions were higher on the left than the right (fig. 3a), at which time the patient did not respond to visual stimuli presented in the right visual field, but did respond to stimuli in the left visual field. Startle responses to threatening stimuli in the right visual field, which appeared on day 19 of treatment, lasted 2 weeks. DW-MRI on day 23 showed decreased high signal intensities in the left temporal and parietal lobes, whereas intensity remained high in the other regions (fig. 3b).

Fig. 1. Patients' appearances before (left) and after (right) quinacrine treatment. **a–c** Patient 1 had an apathetic appearance and unfocused, roving eye movements before treatment (**a**). After treatment, there was eye fixation (**b**) and gaze oriented to auditory stimulus (**c**). **d–f** Patient 3 was listless and apathetic before treatment (**d**). After treatment, she had a well-oriented facial expression (**e**) and purposeful limb movement (**f**).

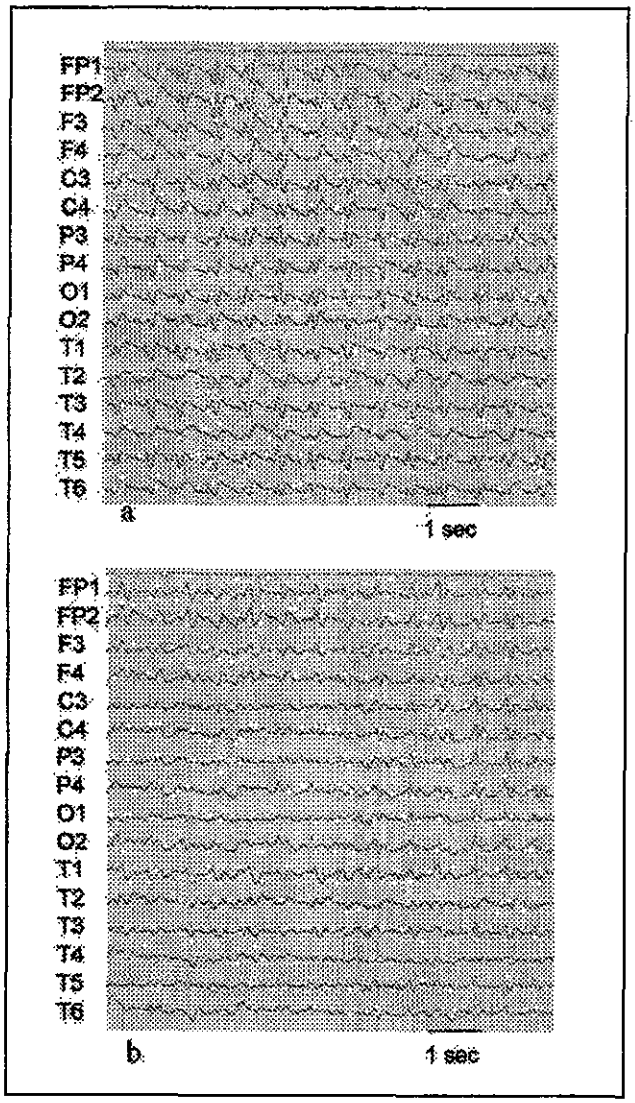

Fig. 2. Electroencephalograms for patient 2 before (**a**) and after (**b**) quinacrine treatment. PSWCs with totally suppressed background activities (**a**) were replaced by fewer periodic patterns and restored background activities after treatment (**b**).

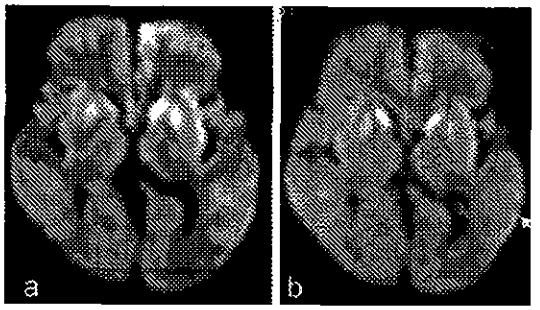

Fig. 3. DW-MRI of patient 2. The right side of each image corresponds to the left side of the brain. High signal intensities were present in the corpus striatum and insular and cingulate gyri on both sides, and in the parietal and temporal lobes before (**a**) and after (**b**) quinacrine treatment. In **b**, the high signal in the left temporoparietal lobes (arrow) is attenuated, whereas signals in the other regions remain unchanged.

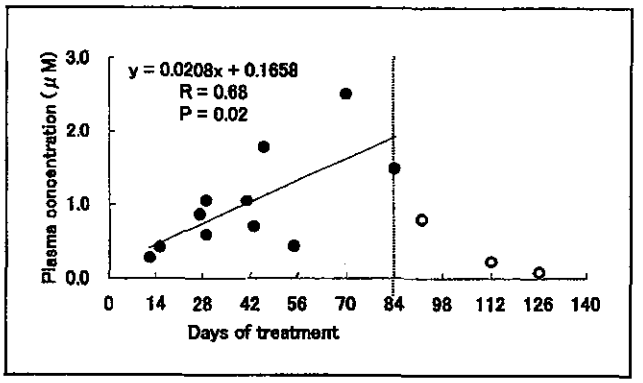

Fig. 4. Plasma concentrations of quinacrine during and after its administration. The concentration increased with the number of days of treatment. Quinacrine was still detectable in the plasma after drug discontinuation on day 84, indicating that it had accumulated in tissues.

Before treatment, patient 3 had high DW-MRI signals in the corpus striatum, cingulate gyrus and left parietal and temporal cortices. These had not changed by the 4th week of treatment, but they disappeared during the 12th week. The other two patients showed diffuse cerebral atrophy without high signals on DW-MRI, which findings did not change after treatment. On the EEGs, patient 1 had PSWCs in the suppressed background before treatment. These disappeared and were replaced by diffuse slow activities of 3–7 Hz during the 2nd week of treatment, but they returned during the 4th week and disappeared thereafter. Patient 3 had PSWCs superimposed on slow background activities, and patient 4 showed diffuse slowing with occasional alpha activities. These features remained unchanged after treatment.

Plasma Concentration of Quinacrine

The plasma concentration of quinacrine increased with the length of administration (fig. 4). It reached 300 n*M* within 14 days and was as high as 2,500 n*M* near the end of the treatment period. Moreover, quinacrine was detectable in the patients' plasma 6 weeks after its discontinuation.

Discussion

In their search for potent agents to treat prion diseases, Doh-ura et al. [4] reported inhibition of PrP^{Sc} accumulation in scrapie-infected neuroblastoma cells by lysosomotropic agents, including quinacrine and cysteine protease inhibitors. These agents may interfere with the conversion of PrP^{c} to PrP^{Sc} at the plasma membrane or along an endocytotic pathway to the lysosomes. Recently, Collins et al. [10] reported that quinacrine did not prolong survival in a murine CJD model. Results of animal experiments, however, depend on the animal species and prion strain. Subcutaneous quinacrine administration prolonged the survival of transgenic mice inoculated with 263K scrapie agents into the brain [Doh-ura, pers. commun.].

We studied four patients, of whom three had clinically probable sCJD and one possibly iatrogenic CJD. All four had improved arousal levels after quinacrine treatment. Other changes in global brain function included decreased frequencies of reflex or action myoclonus (patients 1 and 2) and startle response (patients 2 and 3), and mitigation of the hyperkinetic state (patient 4). Focal brain functions restored were nonpathological laughter (patients 2–4), visual field (patient 2) and voluntary movement (patient 3). These changes might have been due to factors other than quinacrine, e.g. encouragement of contact by family members or caregivers, but this could be excluded for two reasons. Firstly, in Japan, intensive care is customarily given to severely disabled patients who have definitely poor prognoses. As in the case of patient 1, tube feeding is usually initiated and continued for irreversibly disabled patients because family members will not accept the cessation of feeding. The contact provided by family members and caregivers did not change after quinacrine treatment was begun in the present study. Secondly, the changes seen after treatment were transient, lasting 2–8 weeks. Thereafter, the patients' conditions regressed, even during quinacrine administration.

Of the three patients with clinically probable sCJD, transient improvement occurred not only in patients 2 and 3, who were in the early stage, but also in patient 1, who was in the terminal, akinetic mutism stage. This last patient had an improved arousal level associated with directed fixation of the eyes (fig. 1a–c) attributable to the function of the brainstem reticular formation, a structure relatively preserved in the classic, Heidenhain variant of sCJD [11]. The most marked change, seen in patient 2, was the restored response to objects presented in the right visual field. This change was accompanied by decreased DW-MRI signal intensities in the left temporal and parietal lobes. DW-MRI is a new technique that noninvasively images molecular water proton diffusion processes that occur on a micrometer scale [12]. Mittal et al. [13] reported that in CJD, the high-intensity signal areas seen in DW-MRI are correlated with a high degree of spongiform change. They speculated that these changes are the result of the microvacuolation of neuritic processes, heralding spongiform degeneration. Of our four patients, the two who were in the early stage of illness had high signals on DW-MRI that lasted for 2–3 months but which had disappeared 5 months into the illness. Although the exact mechanism is unknown, the immature attenuation of the high signals in the temporal and parietal lobes, which was correlated with clinical changes in patient 2, suggests that the high DW-MRI signals in CJD may represent reversible changes. Decreases in the action myoclonus and startle response in patient 2 were accompanied by decreased PSWCs and increased EEG background activity. These EEG findings suggest that mitigation of the irritable state, which produced a calm appearance, was due to improved cortical function and not to deterioration.

Cognitive function was restored temporarily in patient 4, who had an unusually prolonged course. She may have received contaminated cadaveric dura mater before onset, and her incubation period of 66 months compares with the incubation periods of other Japanese patients (mean incubation period 89 ± 44 months, range 16–193 months) during the CJD outbreak [3]. She had rapidly progressive dementia during the first 2 years of her total, prolonged 6-year course. Some Japanese patients with dura mater-associated CJD may have a clinically variant, longer duration of illness, characterized pathologically by florid-type plaques [14]. The diagnosis in that patient's case has had to be postponed, but quinacrine treatment appears to be beneficial for patients with rapidly progressive dementia and prolonged survival.

Whether the changes found are due to the antiprion effect of quinacrine, as reported in in vitro experiments, is unknown. Therapeutic doses of quinacrine are known to cause psychomotor hyperactivity. The incidence of quinacrine psychosis is reported to be 0.9–4 per 1,000 persons

[15]. Engel et al. [16] administered 2.1–2.8 g of quinacrine to 5 healthy individuals over a 10-day period, doses sufficient to obtain plasma levels exceeding 250 n*M*. Their subjects had various degrees of psychomotor hyperactivity and increases in EEG frequencies. The EEG changes occurred at plasma quinacrine levels of 75–100 n*M* and continued for up to 8 days after discontinuation of the drug. The increased arousal levels in our patients, therefore, may be attributable to the cortical stimulation action of quinacrine, but the mechanism of its direct effect on the central nervous system has yet to be determined.

The plasma concentrations of quinacrine in our patients suggest that a therapeutic dose of 300 mg/day quinacrine may reach the EC_{50} of PrP^{Sc} formation, i.e. 300–400 n*M*, in brain tissues. Quinacrine accumulates progressively in tissues when administered chronically [7]. The lowest concentrations are in the brain, heart and skeletal muscle [7], but tissue to plasma concentration ratios may be very high, as in dog skeletal muscle [8]. The clinical changes in our patients occurred from the 2nd to 8th week of administration, and the plasma concentrations ranged from 300 to 1,000 n*M*. Those concentrations would be sufficient for the drug's accumulation in brain tissues as well as for its action either as a direct cortical stimulant or through its antiprion activity. Cognitive state regression during quinacrine treatment may be due to its toxicity on the brain [6]. We believe that the quinacrine dose should be decreased after the initial loading dose and the plasma concentration of the drug monitored. Although its effectiveness is limited in terms of extent and duration, our findings support undertaking a clinical trial of quinacrine and the search for other chemicals that prevent the accumulation of, or conformational changes in, prion proteins.

Acknowledgment

This study was supported by Research Grant No. 13080901 from the Ministry of Health, Labor and Welfare of Japan.

References

1 Prusiner SB, Hsiao KK: Human prion diseases. Ann Neurol 1994;35:385–395.
2 Will RG, Ironside JW, Zeidler M, Cousens SN, Estibeiro K, Alperovitch A, Poser S, Pocchiari M, Hofman A, Smith PG: A new variant of Creutzfeldt-Jakob disease in the UK. Lancet 1996;347:921–925.
3 Creutzfeldt-Jakob disease associated with cadaveric dura mater grafts – Japan, January 1979–May 1996. MMWR Morb Mortal Wkly Rep 1997;46:1066–1069.
4 Doh-Ura K, Iwaki T, Caughey B: Lysosomotropic agents and cysteine protease inhibitors inhibit scrapie-associated prion protein accumulation. J Virol 2000;74:4894–4897.
5 Korth C, May BC, Cohen FE, Prusiner SB: Acridine and phenothiazine derivatives as pharmacotherapeutics for prion disease. Proc Natl Acad Sci USA 2001;98:9836–9841.
6 Lidz T, Kahn RL: Toxicity of quinacrine (atabrine) for the central nervous system. III. An experimental study on human subjects. Arch Neurol Psychiatry 1946;56:284–299.
7 Rolls IM: Drugs used in the chemotherapy of helminthiasis; in Goodman LS, Gillman A (eds): Pharmacological Basis of Therapeutics, ed 5. New York, Macmillan, 1975, pp 1080–1094.
8 Shannon JA, Earle DP, Brodie BB, Taggart JV, Berliner RW: The pharmacological basis for the rational use of atabrine in the treatment of malaria. J Pharmacol Exp Ther 1944;81:307–330.
9 Brandel J-P, Delasnerie-Lauprêtre N, Laplanche J-L, Hauw J-J, Alpérovitch A: Diagnosis of Creutzfeldt-Jakob disease: Effect of clinical criteria on incidence estimates. Neurology 2000;54:1095–1099.
10 Collins SJ, Lewis V, Brazier M, Hill AF, Fletcher A, Masters C: Quinacrine does not prolong survival in a murine Creutzfeldt-Jakob disease model. Ann Neurol 2002;52:503–506.
11 Parchi P, Giese A, Capellari S, Brown P, Schulz-Schaeffer W, *Windl O, Zerr* I, Budka H, Kopp N, Piccardo P, Poser S, Rojiani A, Streichemberger N, Julien J, Vital C, Ghetti B, Gambetti P, Kretzschmar H: Classification of sporadic Creutzfeldt-Jacob disease based on molecular and phenotypic analysis of 300 subjects. Ann Neurol 1999;46:224–233.
12 Moseley ME, Butts K: Diffusion and perfusion; in Stark DD, Bradley WG Jr (eds): Magnetic Resonance Imaging. St. Louis, Mosby, 1999, p 1515.
13 Mittal S, Farmer P, Kalina P, Kingsley PB, Halperin J: Correlation of diffusion-weighted magnetic resonance imaging with neuropathology in Creutzfeldt-Jakob disease. Arch Neurol 2002;59:128–134.
14 Shimizu S, Hoshi K, Muramoto T, Homma M, Ironside JW, Kuzuhara S, Sato T, Yamamoto T, Kitamoto T: Creutzfeldt-Jakob disease with florid-type plaques after cadaveric dura mater grafting. Arch Neurol 1999;56:357–362.
15 Lindenmayer J-P, Vargas P: Toxic psychosis following use of quinacrine. J Clin Psychiatry 1981;42:162–164.
16 Engel GL, Romano J, Ferris EB: Effect of quinacrine (atabrine) on the central nervous system, clinical and electroencephalographic studies. Arch Neurol Psychiatry 1947;58:337–350.

HIGH LIGHT CME

Clinical diagnosis of MM2-type sporadic Creutzfeldt–Jakob disease

T. Hamaguchi, MD; T. Kitamoto, MD, PhD; T. Sato, MD, PhD; H. Mizusawa, MD, PhD; Y. Nakamura, MD, MPH, FFPHM; M. Noguchi, MD; Y. Furukawa, MD; C. Ishida, MD, PhD; I. Kuji, MD, PhD; K. Mitani, MD; S. Murayama, MD, PhD; T. Kohriyama, MD, PhD; S. Katayama, MD, PhD; M. Yamashita, MD, PhD; T. Yamamoto, MD, PhD; F. Udaka, MD, PhD; A. Kawakami, MD, PhD; Y. Ihara, MD, PhD; T. Nishinaka, MD, PhD; S. Kuroda, MD, PhD; N. Suzuki, MD; Y. Shiga, MD, PhD; H. Arai, MD, PhD; M. Maruyama, MD, PhD; and M. Yamada, MD, PhD

Abstract—*Background:* No method for the clinical diagnosis of MM2-type sporadic Creutzfeldt–Jakob disease (sCJD) has been established except for pathologic examination. *Objective:* To identify a reliable marker for the clinical diagnosis of MM2-type sCJD. *Methods:* CSF, EEG, and neuroimaging studies were performed in eight patients with MM2-type sCJD confirmed by neuropathologic, genetic, and western blot analyses. *Results:* The eight cases were pathologically classified into the cortical (n = 2), thalamic (n = 5), and combined (corticothalamic) (n = 1) forms. The cortical form was characterized by late-onset, slowly progressive dementia, cortical hyperintensity signals on diffusion-weighted imaging (DWI) of brain, and elevated levels of CSF 14-3-3 protein. The thalamic form showed various neurologic manifestations including dementia, ataxia, and pyramidal and extrapyramidal signs with onset at various ages and relatively long disease duration. Characteristic EEG and MRI abnormalities were almost absent. However, all four patients examined with cerebral blood flow (CBF) study using SPECT showed reduction of the CBF in the thalamus as well as the cerebral cortex. The combined form had features of both the cortical and the thalamic forms, showing cortical hyperintensity signals on DWI and hypometabolism of the thalamus on [^{18}F]2-fluoro-2-deoxy-D-glucose PET. *Conclusion:* For the clinical diagnosis of MM2-type sporadic Creutzfeldt–Jakob disease, cortical hyperintensity signals on diffusion-weighted MRI are useful for the cortical form and thalamic hypoperfusion or hypometabolism on cerebral blood flow SPECT or [^{18}F]2-fluoro-2-deoxy-D-glucose PET for the thalamic form.

NEUROLOGY 2005;64:643–648

Sporadic Creutzfeldt–Jakob disease (sCJD) has been classified based on the genotype at polymorphic codon 129 of the prion protein gene (*PrP*) and the physicochemical properties of the pathologic PrP (PrP^{Sc}); various classification systems have been proposed.[1-5] A simple classification[1,2] has been widely accepted and recognizes at least six phenotypes in sCJD: MM1, MV1, VV1, MM2, MV2, and VV2.[3] About 70% of patients with sCJD show the classic CJD phenotype and are mostly classified as MM1 or MV1 types.[3] Their clinical diagnosis relies on the detection of periodic sharp-wave complexes (PSWCs) in EEG, elevated levels of CSF 14-3-3 protein, and typical hyperintensity signals of brain MRI in addition to the classic clinical manifestations.[3,6]

Other phenotypes of sCJD do not present with typical clinical symptoms of classic CJD or PSWCs on EEG.[3,6] Both VV2 and MV2 patients are characterized by ataxia and dementia,[3] and brain MRI and CSF 14-3-3 protein are useful for their clinical diagnosis.[6] As for several reported patients with MM2-type sCJD, some showed positive CSF 14-3-3 protein, but others did not.[6-9] Thus, for MM2 as well as VV1, diagnostic markers have not been established yet.

The clinical features of MM2-type sCJD in some patients were previously reported.[1,3,6,8,10,11] MM2-type sCJD presents with at least two pathologic phenotypes: MM2 cortical and MM2 thalamic forms.[3] In the MM2 cortical phenotype, dementia is a major symptom, and visual or cerebellar signs are usually

From the Department of Neurology and Neurobiology of Aging (Drs. Hamaguchi, Noguchi, Furukawa, and Yamada), Kanazawa University Graduate School of Medical Science, Departments of Neurological Science (Dr. Kitamoto), Neurology (Drs. Suzuki and Shiga), and Geriatric and Complementary Medicine (Drs. Arai and Maruyama), Tohoku University Graduate School of Medicine, Sendai, National Center for Neurology and Psychiatry (Dr. Sato), Kohnodai Hospital, Ichikawa, Department of Neurology and Neurological Science (Dr. Mizusawa), Graduate School, Tokyo Medical and Dental University, Department of Public Health (Dr. Nakamura), Jichi Medical School, Minamikawachi, Department of Neurology (Dr. Ishida), Noto General Hospital, Nanao, Department of Nuclear Medicine (Dr. Kuji), Kanazawa University Hospital, Department of Neurology (Dr. Mitani), Tokyo Metropolitan Geriatric Medical Center, Department of Neuropathology (Dr. Murayama), Tokyo Metropolitan Institute of Gerontology, Department of Neurology (Drs. Kohriyama and Katayama), Hiroshima University Hospital, Department of Neurology (Drs. Yamashita and Yamamoto), Saiseikai Nakatsu Hospital and Medical Center, Osaka, Department of Neurology (Dr. Udaka), Sumitomo Hospital, Osaka, Department of Neurology (Dr. Kawakami), Kaetsu Hospital, Niitsu, Department of Neurology (Drs. Ihara and Nishinaka), Clinical Research Institute, National Hospital Organization Minami-Okayama Medical Center, Okayama, Department of Neuropsychiatry (Dr. Kuroda), Okayama University Graduate School of Medicine and Dentistry, and Creutzfeldt–Jakob Disease Surveillance Committee (Drs. Kitamoto, Sato, Mizusawa, Nakamura, Murayama, Kuroda, Shiga, and Yamada), Japan.

Supported in part by a grant from the Research Committee on Prion Diseases and Slow Virus Infection, Ministry of Health, Welfare, and Labor, Japan.

Received May 24, 2004. Accepted in final form November 1, 2004.

Address correspondence and reprint requests to Dr. M. Yamada, Department of Neurology and Neurobiology of Aging, Kanazawa University Graduate School of Medical Science, 13-1, Takara-machi, Kanazawa 920-8640, Japan; e-mail: m-yamada@med.kanazawa-u.ac.jp

Table 1 Clinical features of eight patients with MM2-type sCJD

Patient no.	Sex	Onset, y	Course, mo	Onset symptoms	Clinical manifestations during illness	Initial diagnosis
1	F	65	Alive (13)	Dementia	Dementia, pyramidal signs, insomnia	CJD
2	F	75	Alive (28)	Depression	Psychiatric symptoms, dementia, myoclonus	CJD
3	M	65	14	Falling to left side	Dementia, myoclonus, cerebellar ataxia, akinetic mutism	CJD
4	F	49	30	Insomnia	Insomnia, dementia, psychiatric symptoms, pyramidal signs, extrapyramidal signs, autonomic symptoms, myoclonus, akinetic mutism	PSP
5	M	64	53	Photophobia	Visual symptoms, extrapyramidal signs, dementia, autonomic symptoms, psychiatric symptoms, myoclonus, akinetic mutism	PSP
6	F	30	73	Blurred vision	Visual symptoms, psychiatric symptoms, cerebellar ataxia, dementia, pyramidal signs, extrapyramidal signs, myoclonus, akinetic mutism	SCD
7	M	71	25	Ataxic gait	Cerebellar ataxia, autonomic symptoms, dementia	SCD
8	M	58	13	Dementia	Dementia, cerebellar ataxia, myoclonus, pyramidal signs, psychiatric symptoms	AD

sCJD = sporadic Creutzfeldt–Jakob disease; PSP = progressive supranuclear palsy; SCD = spinocerebellar degeneration; AD = Alzheimer disease.

absent.[3] There have been no reports of laboratory or neuroimaging studies in MM2 cortical sCJD. In the MM2 thalamic phenotype, the clinical features are insomnia and psychomotor hyperactivity in addition to ataxia and cognitive impairment.[3] This phenotype may be called sporadic fatal insomnia (SFI) because the clinical and pathologic features resemble those of fatal familial insomnia (FFI).[8,10] In the MM2 thalamic form or SFI, no PSWCs on EEG, positive or negative 14-3-3 protein in CSF, and normal brain MRI have been reported.[6,8,10]

Since a report of variant CJD (vCJD) in the United Kingdom in 1996,[12] identification of vCJD has been an important part of the surveillance of prion diseases. The clinical features of vCJD are similar to those of MM2-type sCJD, including young age at onset, long disease duration, absence of PSWCs on EEG, and methionine homozygosity on codon 129 of *PrP* gene.[3,13] Therefore, MM2-type sCJD is important in the differential diagnosis for vCJD.

We have investigated the clinical and neuroimaging features of eight patients with MM2-type sCJD in an attempt to identify a reliable marker for the clinical diagnosis of this type of sCJD.

Methods. *Subjects.* We investigated eight patients with MM2-type sCJD confirmed by neuropathologic, genetic, and western blot analyses. The clinical features, results of EEG, CSF 14-3-3 protein, MRI, cerebral blood flow (CBF) studies using SPECT, and brain glucose metabolism studies using [^{18}F]2-fluoro-2-deoxy-D-glucose (FDG) PET were reviewed. CBF-SPECT using ^{99m}Tc-ethyl cysteinate dimer (^{99m}Tc-ECD) was performed in three (Patients 1, 2, and 8), CBF-SPECT using *N*-isopropyl-*p*-[^{123}I]iodoamphetamine in three (Patients 4, 5, and 6), and FDG-PET in one (Patient 3). MRI, CBF-SPECT, and FDG-PET were evaluated by two neurologists and a neuroradiologist without knowledge of the clinical findings. None of these subjects had a family history of CJD or known exposure to prion contamination in the past.

Analysis of PrP *gene.* DNA was extracted from the blood, and the open reading frame of the *PrP* gene was analyzed as previously described.[14,15]

Neuropathology. The brain tissues were obtained by brain biopsy (Patients 1 and 2) or autopsy (Patients 3 to 8). Brain tissue sections were stained with routine neuropathologic techniques. Immunohistochemistry was performed with a monoclonal antibody to PrP (3F4), as previously described.[16]

Western blot analysis. Brain tissue from the frontal lobe was homogenized, and western blot analysis of protease K-resistant PrP was performed with 3F4 as previously described.[17]

Results. *Clinical features and laboratory and neuroimaging studies.* The clinical features are summarized in table 1 and the laboratory and neuroimaging studies in table 2. The details of the clinical and pathologic features of Patients 5[18] and 6[11] were previously reported, and Patient 8 was included in a previous MRI study.[19] The details of the clinical features of three representative patients (Patients 2, 3, and 8) are described below.

Patient 2. A 75-year-old woman developed forgetfulness and depression. Her mental symptoms gradually deteriorated, and she was admitted to our hospital 14 months after the onset. Neurologically, she showed only dementia (Mini-Mental State Examination 9/30) with depressed mood.

Sixteen months after the onset, the MRI showed gyriform hyperintensity in the bilateral frontal, temporal, parietal, and occipital cortices on diffusion-weighted imaging (DWI) (figure 1A). Less intense and smaller cortical lesions were shown on fluid-attenuated inversion recovery imaging (see figure 1B). On the EEG, diffuse slowing was found without PSWCs. CBF-SPECT using ^{99m}Tc-ECD showed re-

Table 2 Laboratory and neuroimaging findings of eight patients with MM2-type sCJD

	EEG			CSF		Abnormal signals on MRI*				Reduction of CBF or hypometabolism			
Patient no.	Slowing	PSWCs	DD, mo	14-3-3	DD, mo	CO	BG	TH	DD, mo	CO	BG	TH	DD, mo
1	+	−	13	+	9	+	−	−	7	+	−	−	9
2	+	+	27	+	16	+	−	−	16	+	−	−	16
3	+	−	11	±	4	+	−	−	4	+	−	+	4
4	+	−	25	NA		NA				+	−	+	16
5	+	−	42	NA		NA				+	−	+	12
6	+	+	36	NA		−	−	−	58	+	−	+	37
7	+	−	9	+	9	−	−	−	13	NA			
8	+	−	7	±	7	−	−	−	7	+	−	+	7

sCJD = sporadic Creutzfeldt–Jakob disease; CBF = cerebral blood flow; PSWCs = periodic sharp-wave complexes; DD = disease duration at time point when each examination showed the following results: PSWCs on EEG, positive 14-3-3 protein in CSF, abnormal signals on MRI, and reduction of CBF on SPECT or hypometabolism on [^{18}F]2-fluoro-2-deoxy-D-glucose PET or at the time when the last examination was performed if the examinations revealed negative results throughout the clinical course; CO = cortex; BG = basal ganglia; TH = thalamus.

* We judge that abnormal signals are positive on MRI when they are shown on any sequence, such as T1-weighted, T2-weighted, diffusion-weighted, and fluid-attenuated inversion recovery images.

duction of the CBF in the bilateral parietal and temporal cortices (figure 2A). CSF examination revealed an increased level of 14-3-3 protein (28 ng/mL [normal <20 ng/mL]). Although the clinical criteria of sCJD[20] were not fulfilled because of the scarcity of neurologic and EEG abnormalities, CJD was suspected on the basis of MRI and CSF findings.

Twenty-seven months after the onset, the EEG showed PSWCs. Cortical hyperintensity signals on DWI were found to extend to the bilateral frontal regions. ^{99m}Tc-ECD SPECT showed diffuse severe reduction of CBF except in the cerebellum, basal ganglia, and thalamus. To confirm the diagnosis of CJD for participation in a clinical trial of pentosan polysulfate, brain biopsy of the right frontal lobe was performed with her family's consent 28 months after the onset. The patient developed myoclonic movement involving the bilateral hands and was alive 30 months after the onset.

Patient 3. A 65-year-old man developed unsteadiness with a tendency to fall to the left side. Three months after the onset, he showed gait disturbance and dysarthria.

Neurologic examination 4 months after the onset revealed slurred dysarthria, clumsiness of the left upper and lower extremities, and dementia. The EEG was normal. The CSF level of 14-3-3 protein was equivocal. MRI showed gyriform hyperintensity in the bilateral frontal, temporal, parietal, and occipital cortices on DWI. FDG-PET of the brain showed diffuse hypometabolism in the bilateral thalamus and cortices. CJD was suspected as an initial diagnosis.

Thereafter, the patient's symptoms rapidly progressed; he became bedridden and could not communicate 5 months after the onset. Myoclonus of the extremities developed 9 months after the onset. Eleven months after the onset, cortical lesions with hyperintense signals on DWI extended more widely than in the previous study and revealed diffuse, mild atrophy. EEG revealed diffuse slowing without PSWCs. The CSF level of 14-3-3 protein was still equivocal. The patient fell into akinetic mutism 13 months after the onset. He died 14 months after the onset and was autopsied.

Patient 8. A 58-year-old man developed progressive dementia. He showed unsteady gait 5 months after the onset and myoclonic movement in all limbs 6 months after the onset.

Neurologic examination 7 months after the onset revealed dementia, cerebellar ataxia, myoclonic jerking, and exaggerated deep tendon reflexes in all the extremities. Brain MRI, including DWI, and EEG were normal (see figure 1, C and D). CBF-SPECT using ^{99m}Tc-ECD revealed reduction of the CBF in the bilateral thalamus and cortices of the temporal and parietal lobes (see figure 2B). A CSF study disclosed a mild increase of protein concentration (44 mg/dL) and equivocal levels of 14-3-3 protein. The diagnosis was suspicion of Alzheimer disease (AD).

His symptoms gradually deteriorated. He also developed visual hallucinations and confusion 12 months after the onset. Thirteen months after the onset, he died and was autopsied.

PrP *gene analysis.* Analysis of the *PrP* gene revealed no mutation in any of the eight patients. The polymorphic codons showed methionine homozygosity at codon 129 and glutamic acid homozygosity at codon 219 in all the patients.

Neuropathology. Neuropathologically, the biopsy samples from the right frontal cortex of Patients 1 and 2 showed similar pathologic findings: prominent spongiform changes, including large vacuoles, with gliosis, and diffuse granular PrP immunostaining of synaptic type with a perivacuolar pattern.

Autopsies were performed in Patients 3 to 8. The neuropathologic findings of Patients 4 to 8 were similar. Severe neuronal loss and gliosis, but no spongiform changes, were observed in the nuclei of the medial thalamus as well as in the inferior olive. In the thalamus, PrP immunoreactivity was absent in all the patients. In the cerebral cortex, spongiform degeneration was absent in Patient 8 and limited to isolated foci in Patients 4 to 7 mainly in the frontal, pari-

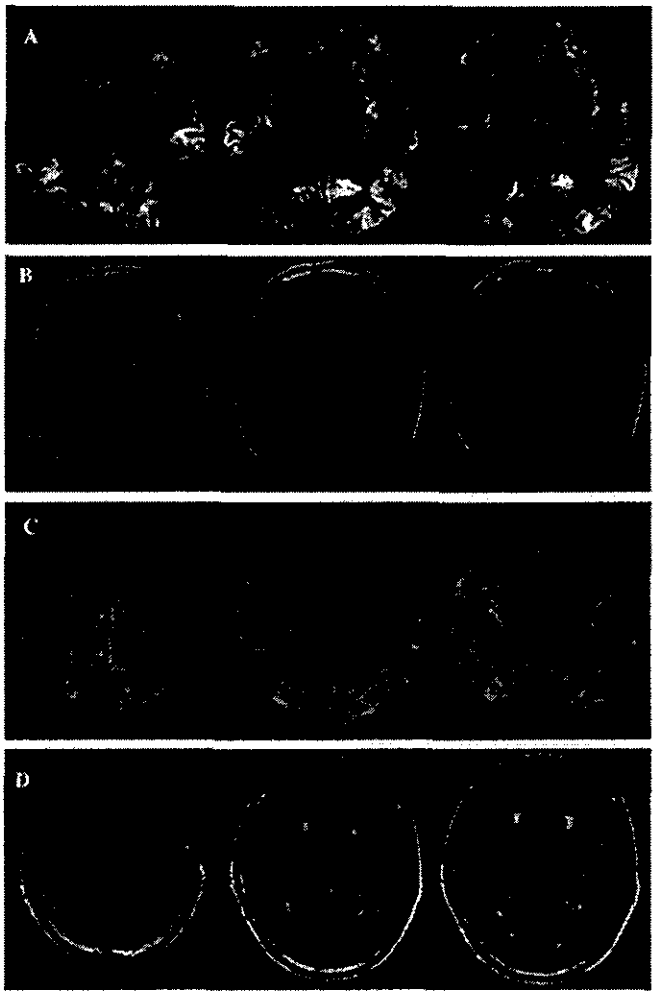

Figure 1. Brain MRI in Patient 2 at 16 months after the onset (A, B) and Patient 8 at 7 months after the onset (C, D). A and C are diffusion-weighted imaging (DWI), and B and D are fluid-attenuated inversion recovery (FLAIR) imaging. In Patient 2, DWI shows hyperintense signals in the bilateral frontal, parietal, and occipital cortices (A), and FLAIR imaging also shows slight hyperintensity signals within the cortical DWI lesions (B). In Patient 8, DWI and FLAIR imaging reveal no distinct abnormal signals in the brain (C, D).

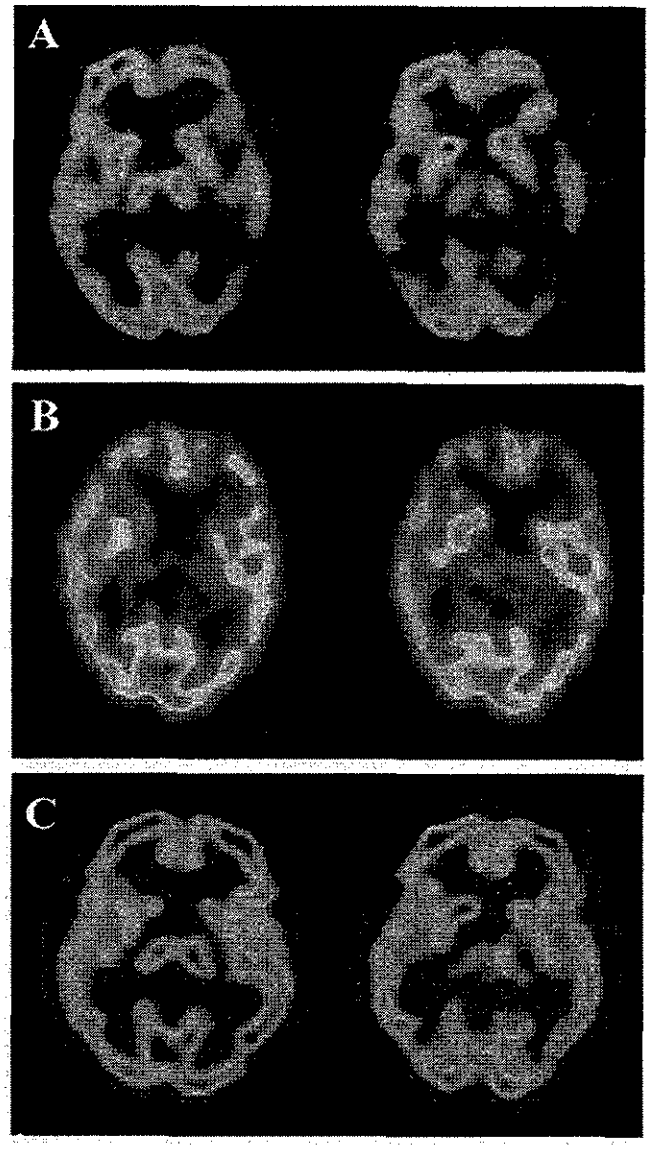

Figure 2. SPECT of cerebral blood flow (CBF) using ^{99m}Tc-ethyl cysteinate dimer in Patient 2 at 16 months after the onset (A), Patient 8 at 7 months after the onset (B), and a normal control subject who was a 67-year-old man without neurologic abnormality or cognitive decline (C). SPECT shows reduction of CBF in the bilateral temporal cortex in Patient 2 (A) and in the bilateral thalamus as well as the temporal cortex in Patient 8 (B) compared with the normal control subject (C).

etal, and temporal lobes, and PrP immunoreactivity was absent in Patients 5 and 8, whereas it was present with a sparse, coarse pattern in Patients 4, 6, and 7. In the subiculum, the neurons were well preserved, and spongiform changes were not evident in any of the patients. In the neostriatum, mild neuronal loss and gliosis were observed in all the patients. In the cerebellum, mild to moderate loss of Purkinje cells was observed, and PrP immunoreactivity was absent in Patients 4, 5, 7, and 8. In Patient 6, Purkinje cells were well preserved, but a small number of plaque-like PrP deposits were observed. In the cerebral white matter, mild or moderate myelin pallor was observed in Patients 4, 5, and 6.

Patient 3 showed the same severe lesions of the medial thalamus and the inferior olive as found in Patients 4 to 8, and PrP immunoreactivity was absent in the thalamus. Furthermore, the cerebral cortex in Patient 3 showed marked spongiform changes in all the layers with diffuse granular PrP staining. The other brain regions showed similar changes to those in Patients 4 to 8.

Western blot analysis. Western blot analysis of the brain samples from all the patients revealed PrP^{Sc} type 2A according to the classification of Parchi et al.[1,2] Compared with the amounts in Patients 1 to 3, only a small amount of PrP^{Sc} type 2A could be detected in Patients 4 to 8.

Discussion. *PrP* gene sequence and western blot analyses revealed that all eight of the patients studied here had MM2-type sCJD. As we analyzed PrP^{Sc} using brain tissue only from the frontal lobe, the

MM2 thalamic sCJD. Our results indicate the usefulness of neuroimaging studies in discrimination between vCJD and MM2-type sCJD.

References

1. Parchi P, Castellani R, Capellari S, et al. Molecular basis of phenotypic variability in sporadic Creutzfeldt–Jakob disease. Ann Neurol 1996;39: 767–778.
2. Parchi P, Capellari S, Chen SG, et al. Typing prion isoforms. Nature 1997;386:232–234.
3. Parchi P, Giese A, Capellari S, et al. Classification of sporadic Creutzfeldt–Jakob disease based on molecular and phenotypic analysis of 300 subjects. Ann Neurol 1999;46:224–233.
4. Collinge J, Sidle KC, Meads J, Ironside J, Hill AF. Molecular analysis of prion strain variation and the aetiology of "new variant" CJD. Nature 1996;383:685–690.
5. Hill AF, Joiner S, Wadsworth JD, et al. Molecular classification of sporadic Creutzfeldt–Jakob disease. Brain 2003;126:1333–1346.
6. Zerr I, Schulz-Schaeffer WJ, Giese A, et al. Current clinical diagnosis in Creutzfeldt–Jakob disease: identification of uncommon variants. Ann Neurol 2000;48:323–329.
7. Otto M, Wiltfang J, Cepek L, et al. Tau protein and 14-3-3 protein in the differential diagnosis of Creutzfeldt–Jakob disease. Neurology 2002; 58:192–197.
8. Parchi P, Capellari S, Chin S, et al. A subtype of sporadic prion disease mimicking fatal familial insomnia. Neurology 1999;52:1757–1763.
9. Castellani RJ, Colucci M, Xie Z, et al. Sensitivity of 14-3-3 protein test varies in subtypes of sporadic Creutzfeldt–Jakob disease. Neurology 2004;63:436–442.
10. Mastrianni JA, Nixon R, Layzer R, et al. Prion protein conformation in a patient with sporadic fatal insomnia. N Engl J Med 1999;340:1630–1638.
11. Yamashita M, Yamamoto T, Nishinaka K, Udaka F, Kameyama M, Kitamoto T. Severe brain atrophy in a case of thalamic variant of sporadic CJD with plaque-like PrP deposition. Neuropathology 2001;21: 138–143.
12. Will RG, Ironside JW, Zeidler M, et al. A new variant of Creutzfeldt–Jakob disease in the UK. Lancet 1996;347:921–925.
13. Will RG, Zeidler M, Stewart GE, et al. Diagnosis of new variant Creutzfeldt–Jakob disease. Ann Neurol 2000;47:575–582.
14. Yamada M, Itoh Y, Fujigasaki H, et al. A missense mutation at codon 105 with codon 129 polymorphism of the prion protein gene in a new variant of Gerstmann–Sträussler–Scheinker disease. Neurology 1993; 43:2723–2724.
15. Kitamoto T, Ohta M, Doh-ura K, Hitoshi S, Terao Y, Tateishi J. Novel missense variants of prion protein in Creutzfeldt–Jakob disease or Gerstmann–Sträusller syndrome. Biochem Biophys Res Commun 1993;191: 709–714.
16. Kitamoto T, Shin RW, Doh-ura K, et al. Abnormal isoform of prion protein accumulates in the synaptic structures of the central nervous system in patients with Creutzfeldt–Jakob disease. Am J Pathol 1992; 140:1285–1294.
17. Shimizu S, Hoshi K, Muramoto T, et al. Creutzfeldt–Jakob disease with florid-type plaques after cadaveric dura mater grafting. Arch Neurol 1999;56:357–362.
18. Kawasaki K, Wakabayashi K, Kawakami A, et al. Thalamic form of Creutzfeldt–Jakob disease or fatal insomnia? Report of a sporadic case with normal prion protein genotype. Acta Neuropathol 1997;93:317–322.
19. Shiga Y, Miyazawa K, Sato S, et al. Diffusion-weighted MRI abnormalities as an early diagnostic marker for Creutzfeldt–Jakob disease. Neurology 2004;63:443–449.
20. Masters CL, Harris JO, Gajdusek DC, Gibbs CJ Jr, Bernoulli C, Asher DM. Creutzfeldt–Jakob disease: patterns of worldwide occurrence and the significance of familial and sporadic clustering. Ann Neurol 1979;5: 177–188.
21. Puoti G, Giaccone G, Rossi G, Canciani B, Bugiani O, Tagliavini F. Sporadic Creutzfeldt–Jakob disease: co-occurrence of different types of PrP^{Sc} in the same brain. Neurology 1999;53:2173–2176.
22. Demaerel P, Sciot R, Robberecht W, et al. Accuracy of diffusion-weighted MR imaging in the diagnosis of sporadic Creutzfeldt–Jakob disease. J Neurol 2003;250:222–225.
23. Schaefer PW, Grant PE, Gonzalez RG. Diffusion-weighted MR imaging of the brain. Radiology 2000;217:331–345.
24. Kolb SJ, Costello F, Lee AG, et al. Distinguishing ischemic stroke from the stroke-like lesions of MELAS using apparent diffusion coefficient mapping. J Neurol Sci 2003;216:11–15.
25. Bozzao A, Floris R, Baviera ME, Apruzzese A, Simonetti G. Diffusion and perfusion MR imaging in cases of Alzheimer's disease: correlations with cortical atrophy and lesion load. AJNR Am J Neuroradiol 2001;22: 1030–1036.
26. de Silva R, Patterson J, Hadley D, Russell A, Turner M, Zeidler M. Single photon emission computed tomography in the identification of new variant Creutzfeldt–Jakob disease: case reports. Br Med J 1998; 316:593–594.
27. Matsuda M, Tabata K, Hattori T, Miki J, Ikeda S. Brain SPECT with ^{123}I-IMP for the early diagnosis of Creutzfeldt–Jakob disease. J Neurol Sci 2001;183:5–12.
28. Perani D, Cortelli P, Lucignani G, et al. [18F] FDG PET in fatal familial insomnia: the functional effects of thalamic lesions. Neurology 1993; 43:2565–2569.
29. Cortelli P, Perani D, Parchi P, et al. Cerebral metabolism in fatal familial insomnia: relation to duration, neuropathology, and distribution of protease-resistant prion protein. Neurology 1997;49:126–133.
30. Ishii K. Clinical application of positron emission tomography for diagnosis of dementia. Ann Nucl Med 2002;16:515–525.
31. Blin J, Baron JC, Dubois B, et al. Positron emission tomography study in progressive supranuclear palsy. Arch Neurol 1990;47:747–752.
32. Van Laere K, Santens P, Bosman T, De Reuck J, Mortelmans L, Dierckx R. Statistical parametric mapping of 99mTc-ECD SPECT in idiopathic Parkinson's disease and multiple system atrophy with predominant parkinsonian features: correlation with clinical parameters. J Nuc Med 2004;45:933–942.
33. Zeidler M, Sellar RJ, Collie DA, et al. The pulvinar sign on magnetic resonance imaging in variant Creutzfeldt–Jakob disease. Lancet 2000; 355:1412–1418.
34. Collie DA, Summers DM, Sellar RJ, et al. Diagnosing variant Creutzfeldt–Jakob disease with the pulvinar sign: MR imaging findings in 86 neuropathologically confirmed cases. AJNR Am J Neuroradiol 2003;24:1560–1569.

possibility of the coexistence of type 1 and type 2 of PrP^{Sc} in a single brain[3,21] cannot be ruled out. However, we consider it reasonable to classify our patients as having MM2-type sCJD, because the clinical and pathologic phenotypes of our patients were consistent with those of previously reported cases.[3,8,10] Neuropathologically, Patients 1 and 2 were classified as having the cortical form[3] and Patients 4 to 8 the thalamic form.[3] As Patient 3 presented with features of both the cortical and the thalamic forms, this case could be designated as the combined (corticothalamic) form. Because complete neuropathologic examination was not performed in Patients 1 and 2, the possibility that they had the combined form cannot be ruled out.

Patients 1 and 2 with the MM2 cortical form presented with late-onset, slowly progressive dementia (table 1). PSWCs on EEG were absent in the early stage (table 2). These features resembled those of previously reported MM2 cortical cases.[3] Our patients did not fulfill the clinical criteria for sCJD because of the scarcity of clinical symptoms.[20] Importantly, cortical hyperintensity signals on DWI (see table 2), which have been reported to be useful for diagnosis of sCJD,[19,22,23] easily led us to a possible diagnosis of CJD. The basal ganglia and thalamus in these cases showed no hyperintensity signals on MRI. Increased CSF levels of 14-3-3 protein supported the diagnosis (see table 2). As the MM2 cortical form frequently shows slowly progressive dementia without other neurologic abnormalities, AD and dementia with Levy bodies are important for differential diagnosis. Cortical hyperintensity signals on DWI are found in acute ischemic stroke,[23] herpes simplex meningoencephalitis,[22,23] posttraumatic contusion,[22,23] postictal change,[22] and MELAS (mitochondrial myopathy, encephalopathy, lactic acidosis, and stroke-like episodes)[24]; however, they are not observed in AD[25] or dementia with Lewy bodies.[19] We propose the following diagnostic criteria for MM2 cortical sCJD: 1) progressive dementia, 2) cortical hyperintensity signals on DWI, and 3) increased CSF 14-3-3 protein level, with exclusion of the other dementias, including other types of prion diseases. Other neuropsychiatric abnormalities than dementia or PSWCs on EEG are not necessarily required.

In the cases of MM2 thalamic form, the age at onset ranged from 30 to 71 years and the duration of the clinical course from 13 to 73 months (see table 1). Clinical manifestations included psychiatric symptoms, dementia, cerebellar ataxia, insomnia, and autonomic failure (see table 1). As for the outstanding features of FFI and SFI, insomnia was found in only one patient (Patient 4), and autonomic symptoms were found in three patients (Patients 4, 5, and 7). EEG showed no PSWCs except in one patient (Patient 6) who showed PSWCs in the very late stage (see table 2). These features resemble those of previously reported patients with MM2 thalamic[3] or SFI.[8,10] Brain MRI, including DWI, was almost normal in the MM2 thalamic patients except for brain atrophy or white matter changes in the late stage (see table 2). These features are consistent with previously those of reported patients with SFI.[8,10] In our study, of two patients tested for CSF 14-3-3 protein, one was positive and the other was equivocal (see table 2). In the literature, to our knowledge, there are reports of four patients with MM2 thalamic sCJD who have been examined for CSF 14-3-3 protein: The examination was positive in one[6] and negative in three.[7,8] Considering those reports together with our results, we cannot conclude that the CSF 14-3-3 protein is sensitive enough to diagnose MM2 thalamic sCJD. As the initial clinical diagnosis, progressive supranuclear palsy (PSP), spinocerebellar degeneration (SCD), or AD had been suspected (see table 1), indicating considerable difficulty in the clinical diagnosis of the MM2 thalamic form. However, our review of CBF-SPECT studies revealed characteristic findings of reduction of the CBF in the bilateral thalamus as well as the cerebral cortex from relatively early stages (see table 2). In previous reports of CBF-SPECT studies in CJD patients, reduction of CBF on visual inspection was found in various regions of the cerebral cortex but not in the thalamus.[26,27] There have been no reports about CBF-SPECT in MM2 thalamic sCJD. In FDG-PET studies, hypometabolism of the thalamus and cortex has been reported in a patient with SFI[10] or in some patients with FFI.[28,29] CBF and glucose metabolism in the thalamus are relatively preserved in AD.[30] In PSP, significant reduction of glucose metabolism is not detected in the thalamus but is detected in the frontal cortex by using region/occipital metabolic ratios.[31] In multiple system atrophy, a phenotype of sporadic SCD, reduction of the CBF in the thalamus was reported; however, significant reduction of the CBF was also detected in the dorsal putamen.[32] Our patients with MM2 thalamic sCJD showed no reduction of the CBF in the putamen (see figure 2B). Our results clearly indicate that reduction of CBF as well as hypometabolism in the bilateral thalamus, with their preservation in the putamen, would be a particularly useful diagnostic marker for the MM2 thalamic sCJD.

Interestingly, in the patient with the MM2 combined (corticothalamic) form (Patient 3), the neuroimaging studies showed features of both MM2 cortical and thalamic forms, that is, hyperintense signals in the cortex on DWI and thalamic hypometabolism on FDG-PET (see table 2), consistent with the pathologic findings in this patient.

Hyperintensity of the bilateral thalamus (the pulvinar sign) on MRI has been established to be a useful diagnostic marker for vCJD.[33,34] However, no abnormal signals in the pulvinar MRI can be detected in MM2-type sCJD, as shown in the current study and in previous reports.[8,10] A CBF-SPECT study in two patients with vCJD demonstrated widespread reduction of the CBF in the cerebral cortices but no obvious involvement of the thalami.[26] These CBF-SPECT features are different from those in